processes

MDPI

Article

In Situ Deposition of Green Silver Nanoparticles on Urinary Catheters under Photo-Irradiation for Antibacterial Properties

Fueangfahkan Chutrakulwong [1], Kheamrutai Thamaphat [1,*], Sukon Tantipaibulvut [2] and Pichet Limsuwan [1]

[1] Green Synthesis and Application Laboratory, Applied Science and Engineering for Social Solution Research Unit, Department of Physics, Faculty of Science, King Mongkut's University of Technology Thonburi, Bangkok 10140, Thailand; puy_wizard@hotmail.com (F.C.); pichetlaser@gmail.com (P.L.)

[2] Department of Microbiology, Faculty of Science, King Mongkut's University of Technology Thonburi, Bangkok 10140, Thailand; sukon.tan@mail.kmutt.ac.th

* Correspondence: kheamrutai.tha@kmutt.ac.th; Tel.: +66-2470-8961; Fax: +66-2427-8785

Received: 22 November 2020; Accepted: 8 December 2020; Published: 11 December 2020

Abstract: Urinary tract infections, especially catheter-associated urinary tract infections (CAUTIs), are the most common type of nosocomial infections. Patients with chronic indwelling urinary catheters have a higher risk of infection due to biofilm formation on the urinary catheter surface. Therefore, in this work, a novel, cost-effective antimicrobial urinary catheter was developed using green technology. Silver nanoparticles (AgNPs) synthesized from Mon Thong durian rind waste were used as an antimicrobial agent for the prevention of infection. Flavonoids, phenolic compounds, and glucose extracted from durian rind were used as a reducing agent to reduce the Ag^+ dissolved in $AgNO_3$ solution to form non-aggregated AgNPs under light irradiation. The AgNPs were simultaneously synthesized and coated on the inner and outer surfaces of silicone indwelling urinary catheters using the dip coating method. The results showed that the antimicrobial urinary catheter fabricated using a 0.3 mM $AgNO_3$ concentration and 48 h coating time gave the highest antibacterial activity. The as-prepared spherical AgNPs with an average diameter of 9.1 ± 0.4 nm formed on catheter surfaces in a monolayer approximately 1.3 μm thick corresponding to a 0.712 mg/cm^2 silver content. The AgNP layer was found to damage and almost completely inhibit the growth of *Escherichia coli* cells with antibacterial activity by 91%, equivalent to the commercial, high-price antimicrobial urinary catheter. The cumulative amount of silver released from the coated catheter through artificial urine over 10 days was about 0.040 μg/mL, which is less than the silver content that causes tissue and organ toxicity at 44 μg/mL. Thus, we concluded that the developed antimicrobial urinary catheter was useful in reducing the risk of infectious complications in patients with indwelling catheters.

Keywords: antimicrobial urinary catheter; catheter-associated urinary tract infection; silver nanoparticle; durian rind; green synthesis

1. Introduction

A urinary catheter is one of the most essential medical devices with the aim to drain urine from the bladder on an intermittent or indwelling catheterization. Insertion of the urinary catheters in patients in hospitals, nursing homes, healthcare service units, or elderly residents may carry microorganisms originating from the patients' endogenous flora on the skin, mucous membranes, or hollow viscera, or from exogenous sources, such as other patients, medical instruments, healthcare workers, and the environment, into the bladder or kidneys. These lead to catheter-associated urinary tract infections (CAUTIs) [1]. The uropathogens involved with CAUTIs are fungi, like *Candida* species, and both

Gram-positive and Gram-negative bacteria, such as *Escherichia coli* (*E. coli*), *Klebsiella pneumoniae* (*K. pneumoniae*), *Staphylococcus aureus* (*S. aureus*), *Pseudomonas aeruginosa* (*P. aeruginosa*), *Proteus mirabillis* (*P. mirabillis*), and *Enterococcus faecalis* (*E. faecalis*) [2–5]. Among them, the most prevalent CAUTI uropathogenic organisms are *E. coli* as well as *K. pneumonia* in 30.5% of infections, followed by *P. aeruginosa* as well as *Candida* species in 16.6%, and a small proportion of *S. aureus* [2,6].

CAUTIs are one of the most common type of nosocomial infections in hospitals or healthcare service units, accounting for approximately 40–50% of nosocomial infection worldwide [6–8]. The risk of infection for each patient depends on the gender, age, illness severity, and particularly the duration of catheterization, which is a main factor for bacteriuria enhancement with a daily increase of 3–10% [7,9]. Most patients who require the indwelling urinary catheter for a short-term catheterization (1–28 days) have asymptomatic bacteriuria. However, less than 5% of these patients encounter a bloodstream infection [10,11]. Whereas all patients undergoing continuous long-term catheterization for longer than a month have experienced symptoms, such as fever, bacteremia, and acute pyelonephritis to death with mortality rate of 10–15% even when providing excellent care [10,12].

The pathogenesis of CAUTIs result from the biofilm formation on indwelling catheter surfaces [13]. A biofilm is an aggregation of microorganisms sheathed in the matrix of extracellular polymeric substances consisting of DNA, proteins, lipids, and lipopolysaccharides. They are initially produced from the attachment of free-swimming (planktonic) bacterium on the indwelling catheter surface and eventually lead to microbial infective biofilm formation [14,15]. For CAUTI prevention, several strategies have been developed to kill planktonic bacteria or inhibit microbial adhesion on the surface using bioactive coatings [3,4,7,12,15–20]. The most common approach relies on using antibiotics; however, these are only effective against bacterial infection in short-term catheterization [10].

Recently, silver nanoparticles (AgNPs) have been of particular interest as they exhibit efficient long-term toxicity to a wide range of various bacteria, fungi, yeast, and antibiotic-resistant microorganisms [21]. However, they offer low toxicity to mammalian cells [12,15,22]. Based on these distinctive excellent properties of AgNPs, they have been widely used for antimicrobial applications in numerous fields, like fabric, food storage, cosmetics, medicine, and medical devices [21,23,24]. The antimicrobial activity of AgNPs depends on their shape and size. The spherical shape with the smallest size exhibits the strongest antimicrobial activity against *E. coli* in comparison to the triangular and larger spherical shape due to the large surface to volume ratio and high-atomic-density {111} facets [25,26].

In particular, the AgNPs with a spherical particle diameter in the range of 1–10 nm have the highest effectiveness for a direct interaction with the bacterial cell surface [15,27,28]. Consequently, a variety of AgNP synthetic methods, including physical, chemical, and biological methods, developed in recent years emphasizes controlling the size, shape, and stability of AgNPs. Among those methods, the chemical method provides colloidal AgNPs with good uniform size distribution and dispersion stability. Unfortunately, it also produces a large amount of chemical waste resulting in environmental pollution [29]. The biological method based on using various biological organisms, like microorganisms and parts of plants, has therefore emerged to synthesize AgNPs using a green chemistry approach with simple steps and less toxicity [30].

From our previous work, we successfully produced excellent long-term dispersion stability of spherical AgNPs with an absolute zeta potential value of 53.2 ± 1.6 mV using the aqueous extraction from waste durian rinds as a green source of reducing and capping agents under photo-irradiation [31]. Consequently, in the present work our challenge was to use photo-assisted synthesis to produce size-controlled AgNPs with a diameter of less than 10 nm from waste durian rinds for facile in situ deposition on a commercial silicone urinary catheter to achieve an antimicrobial layer for overcoming the CAUTI problem. The silver concentrations on the coated catheter and their silver-releasing properties were determined. In addition, the antimicrobial activity of AgNPs coated on catheters against the most common CAUTI, uropathogenic *E. coli*, was compared with the commercially available antimicrobial urinary catheter.

2. Materials and Methods

2.1. In Situ AgNPs Deposition on the Silicone Urinary Catheter

A silicone coated latex Foley catheter (18 Fr., 6 mm outer diameter) manufactured by Kendall International, Inc. was cut into small pieces of 2 cm in length. They were cleaned with ethanol, dried under a stream of nitrogen gas, and kept in an airtight plastic container for use throughout the experimental research.

To study the in situ AgNPs coating process, the cleaned catheter pieces were quickly rinsed with acetone and then immersed in 30 mL of the white part of Mon Thong durian rind (mesocarp and endocarp layers) extract contained in a 250-mL flask. The durian rind extraction procedure was carried out according to previous work [31]. After that, 0.3 mM $AgNO_3$ (POCH) solution was slowly added to the extract in the ratio of 1:1, and the pH value of the mixture was adjusted to 8.5 using 0.1 M NaOH (Ajax). Later, the flask was immediately placed on a magnetic stirrer under a dimmable 20 W compact fluorescent light bulb in an assembled opaque system to block the external light as shown in Figure 1. The catheter pieces were incubated in a mixture under a magnetic stirring rate of 390 rpm and a light exposure with the light intensity of 13,430 lx to induce the nucleation, growth, and deposition of AgNPs on the catheter surface. The temperature of the mixture was maintained constant at 25 ± 1 °C throughout the process.

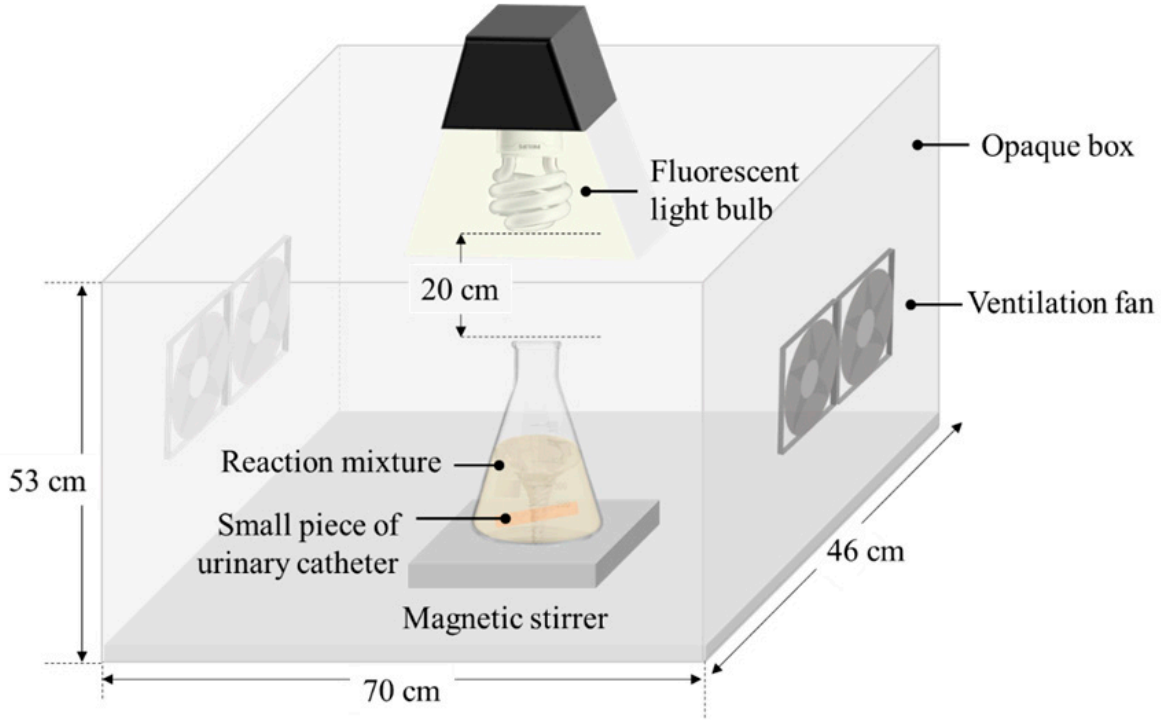

Figure 1. Schematic illustration of the experimental setup for the in situ silver nanoparticle (AgNP) coating on a silicone urinary catheter under photo-irradiation.

After incubation under the light irradiation, the catheters were taken out and heated at 53 ± 1 °C for 10 min in a hot air oven for thermal curing. Then, the catheters were rinsed successively with de-ionized water, ethanol, and de-ionized water and dried with nitrogen gas. The coating process was repeated according to the above-mentioned procedure with different photo-irradiation times (or coating times) of 1, 3, 6, 9, 12, 24, and 48 h. For each irradiation time, the experiment was completed in triplicate.

2.2. Characterization of AgNPs

To confirm the formation of AgNPs, the colloidal solution of AgNPs was partially collected from a mixture at different irradiation times to observe the UV-Vis absorption spectra in the wavelength range of 300–800 nm and the morphology and particle size using an AvaSpec-2048 Fiber Optic Spectrometer and a JEOL-2100 transmission electron microscope (TEM) operated at 200 kV. The topography and thickness of AgNPs covered on a coated catheter surface were investigated by field emission scanning electron microscope (FESEM) using a HITACHI SU8030 operating at an ultra-low accelerating voltage of 1.0 kV. A PerkinElmer AAnalyst 300 atomic absorption spectrometer (AAS) was used to confirm the existence of silver and quantitatively evaluate the silver contents on a coated catheter surface by measuring the absorbance at a wavelength of 328.1 nm.

2.3. Investigation of Antibacterial Activity

The quantitative bactericidal analysis of the green AgNPs in situ coated catheters on the bacterial suspension was performed using evaluation of the surviving cell by a colony forming unit test. The Gram-negative bacteria *E. coli* (ATCC 25922) was selected to be tested due to being the most common pathogen of CAUTIs. Prior to bactericidal testing, the catheter samples were sterilized using an autoclave at 121 °C for 15 min. Then, three coated catheter samples obtained from the same deposition condition were placed in a test tube containing 10^6 CFU/mL of a log-phase *E. coli* suspended in 4.5 mL of phosphate buffer solution (PBS) with pH 7.5. The tubes were then transferred to incubate under aerobic conditions at 37 °C for 48 h.

After incubation, the catheters were gently removed from a cell suspension and the supernatant was randomly collected to examine the effect of AgNPs on bacterial cells. The number of viable cells (free-floating bacteria) was determined using a conventional plate count method, while the phenomenon of bacterial cell death was observed by TEM (Hitachi, HT-7700) operated at an accelerating voltage of 120 kV. The bacterial sample preparation for TEM was as follows.

Briefly, the bacterial cells were soaked in 2.5% glutaraldehyde at 4 °C for 4 h, washed three times with 0.1 M PBS, and then kept in 0.1 M PBS at 4 °C. Then, the sample was cut into small cubes (~1 mm^3), fixed with 1% osmium tetroxide in PBS at 4 °C for 2 h, and washed three times with 0.1 M PBS (4 °C), followed by sequential gradient dehydration from 70% to 100% ethyl alcohol and embedding in pure Araldite 502 resin. Subsequently, the biological specimen was stained with saturated uranyl acetate in 70% methanol and 0.1% lead citrate in water for at least 15 min and mounted on a copper grid for TEM observation. In the experiment, a tube containing a non-coated catheter was used as a negative control for comparison. The antibacterial efficacy of the developed antibacterial catheters was compared in parallel with a commercial Dover^{TM} silver-coated silicone Foley catheter manufactured by Covidien.

2.4. Silver Release Analysis

To assess the in vitro silver released from a green AgNP-coated catheter, the developed antibacterial catheter in 2-cm-long segments was completely immersed in 2 mL of sterilized artificial urine (pH 7.4) prepared according to DIN EN1616: 1999 standard procedure [32] and incubated at 37 °C for 24 h. Every day for 10 days, the artificial urine was collected and replaced with fresh sterilized artificial urine. The amounts of released silver in the collected urine were determined by an inductively coupled plasma optical emission spectrometer (ICP-OES, PerkinElmer, Optima 8000) and expressed in μg/day.

2.5. Statistical Analysis

Statistical analysis was carried out using SPSS Statistics 17.0. The reported data were expressed as the mean ± standard deviation of three independent experiments.

3. Results and Discussion

3.1. Effect of the Photo-Irradiation Time on the AgNP Formation

In this work, the antibacterial urinary catheters were developed by in situ deposition of AgNPs under photo-irradiation. The flavonoids, phenolic compounds, and glucose present in the white part of durian rind extract were served as reducing agents to reduce silver ions (Ag^+) into a zero-valent state (Ag^0) followed by nucleation and growth to AgNPs. The proteins dominated in the extract were served as excellent particle-stabilizing agents in the formation of AgNP dispersion with high stability by using the visible light irradiation to accelerate the synthetic reaction [31] as shown in Figure 2. The as-prepared green AgNPs were simultaneously in situ deposited on both the extraluminal and intraluminal surfaces of a silicone urinary catheter. Figure 3 shows the photographic images of catheters coated with AgNPs at different photo-irradiation times.

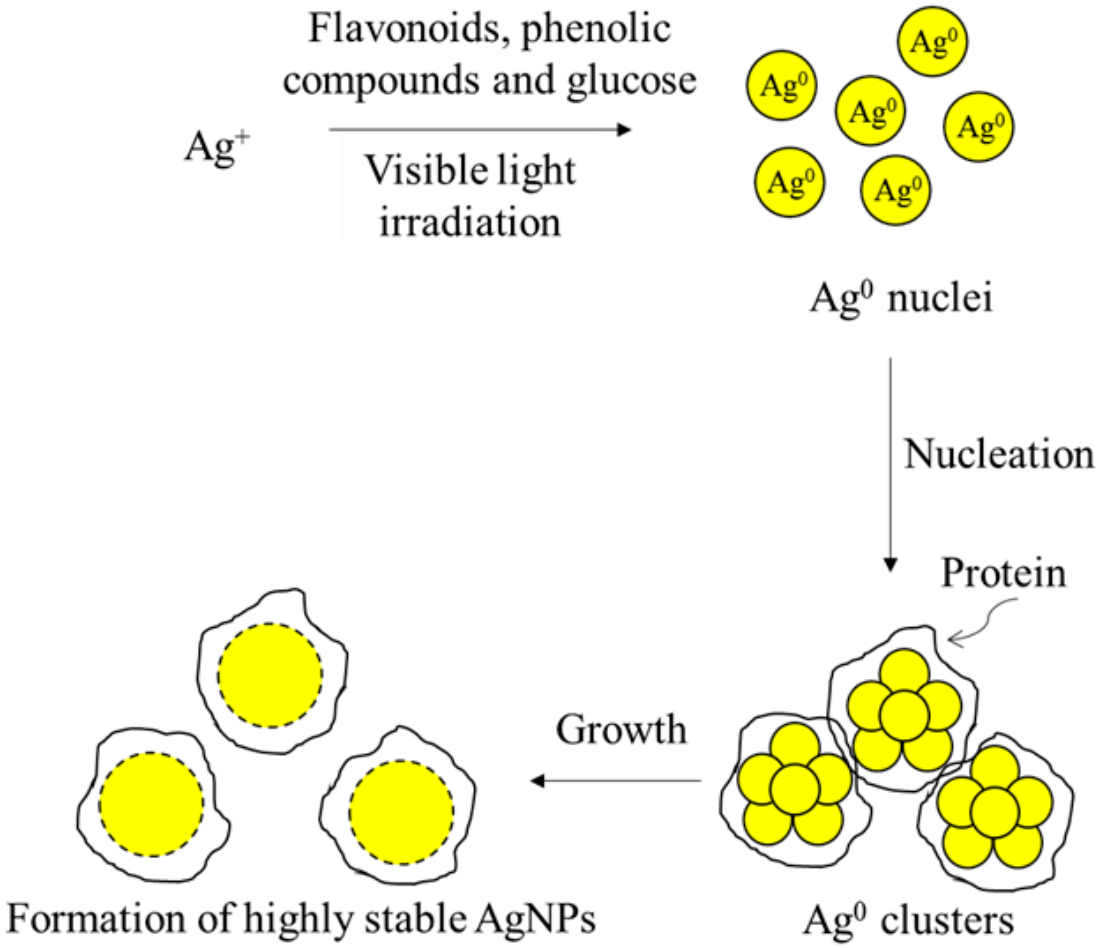

Figure 2. Schematic diagram of AgNP formation via a photo-assisted green chemistry approach using $AgNO_3$ solution and durian rind extract as a natural precursor.

As depicted in Figure 3, we observed that the color of the ordinary silicone urinary catheter turned from bright yellow to brown and became darker with the increasing irradiation time, indicating the formation and instantaneous deposition of AgNPs on the catheter surfaces with longer irradiation times resulting in higher deposited silver concentrations. This appearance concurrently occurred with the change in the color of a mixture of durian rind extract and $AgNO_3$ solution after incubating under the visible light for different times, as displayed in Figure 4. This is because the surface plasmon oscillated at the same frequency as an electric field component of the incident light and is referred as a surface plasmon resonance (SPR) phenomenon [33]. The colloidal AgNPs suspensions as illustrated

in Figure 4 exhibited similar UV-vis absorption spectra with a SPR peak located at a wavelength of approximately 424 nm (Figure 5) providing strong evidence to confirm the presence of AgNPs.

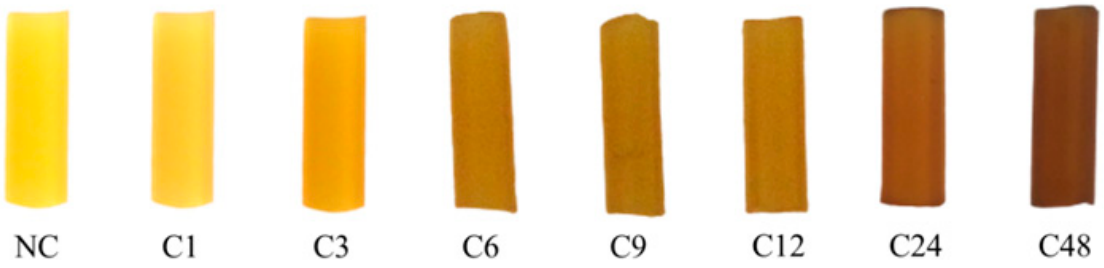

Figure 3. Images of the non-coated catheter (NC) and AgNP-coated catheters achieved from in situ coating within 1 h (C1), 3 h (C3), 6 h (C6), 9 h (C9), 12 h (C12), 24 h (C24), and 48 h (C48).

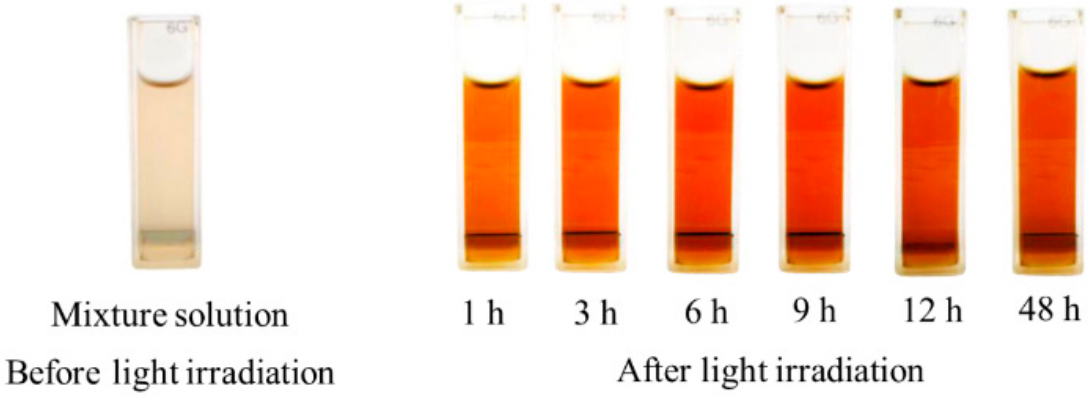

Figure 4. Photographs showing the color of the resultant colloidal AgNP suspensions after visible light exposure with the light intensity of 13,430 lx for 1–48 h.

Figure 5 reveals no significant difference in the SPR peak position. The absorbance intensity slightly increased when increasing the irradiation time, which principally occurred as a result of producing more particles with almost the same particle diameter size [34] corresponding to the TEM observations. The representative results of the TEM investigation are presented in Figure 6, which shows that the AgNPs were formed in spherical shapes with an average diameter of 9.1 ± 0.4 nm. These AgNPs moved to establish a thin layer on both the inner and outer catheter surfaces by in situ deposition. The surface morphology of the urinary catheter before and after AgNP coatings was investigated using FESEM, and the selected cross-sectional FESEM images are represented in Figure 7. These reveal that the smooth catheter surfaces after coating for 6, 12, and 48 h were sheltered by a rough single-layer of AgNPs with thicknesses of approximately 0.3, 0.6, and 1.3 µm corresponding to silver contents of 0.550, 0.637, and 0.712 mg/cm^2, respectively.

3.2. *Bactericidal Activity of Developed Antibacterial Urinary Catheters*

In the present research, the AgNP-coated urinary catheters developed under photo-irradiation times of 3, 12, 24, and 48 h were tested to determine the antibacterial efficiency against non-adherent *E. coli* with an initial concentration of 10^6 CFU/mL (indicative of true CAUTIs [35]) compared to the commercial Dover^{TM} silver-coated silicone catheter, designated CC. Using the counting of colony-forming units on agar plates, the results, as displayed in Figure 8, indicated that a few bacterial colonies were observed in C48, which nearly equaled the commercial one, whereas the non-coated catheter yielded many colonies that spread over the plate. The bacterial killing activity was found to be increased with an increase in the silver concentration deposited on the catheter as shown in Table 1.

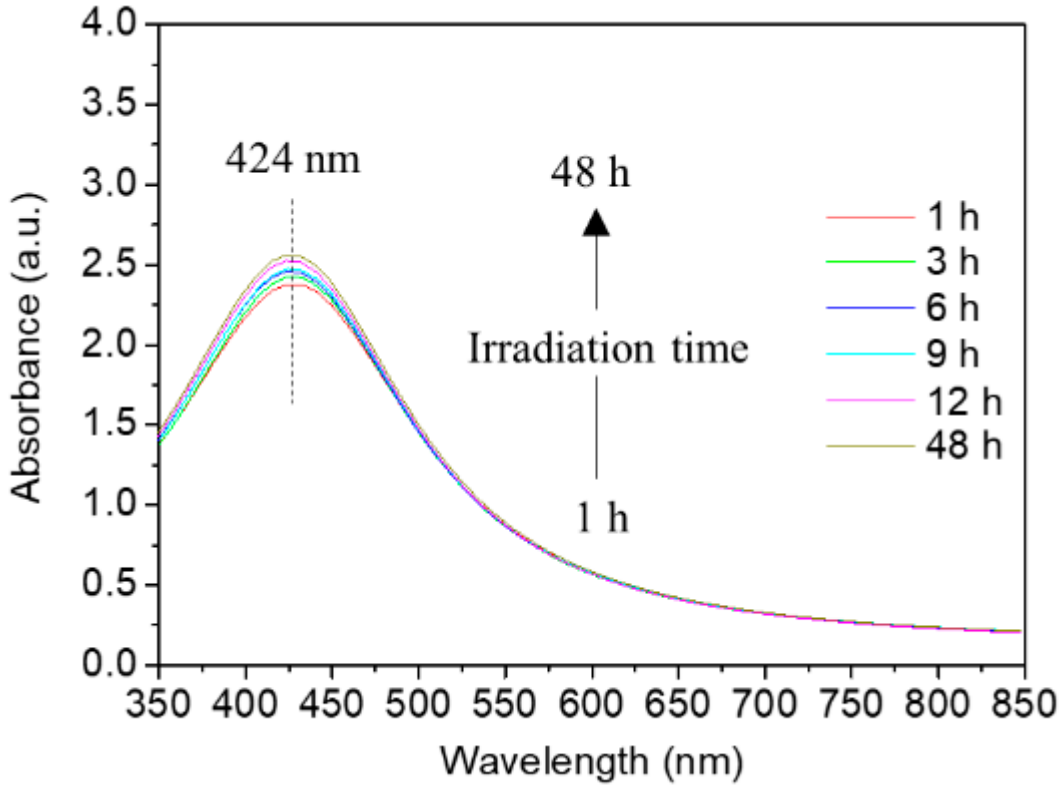

Figure 5. UV-Vis spectra of the green AgNP colloids synthesized under light exposure with the light intensity of 13,430 lx at different irradiation times.

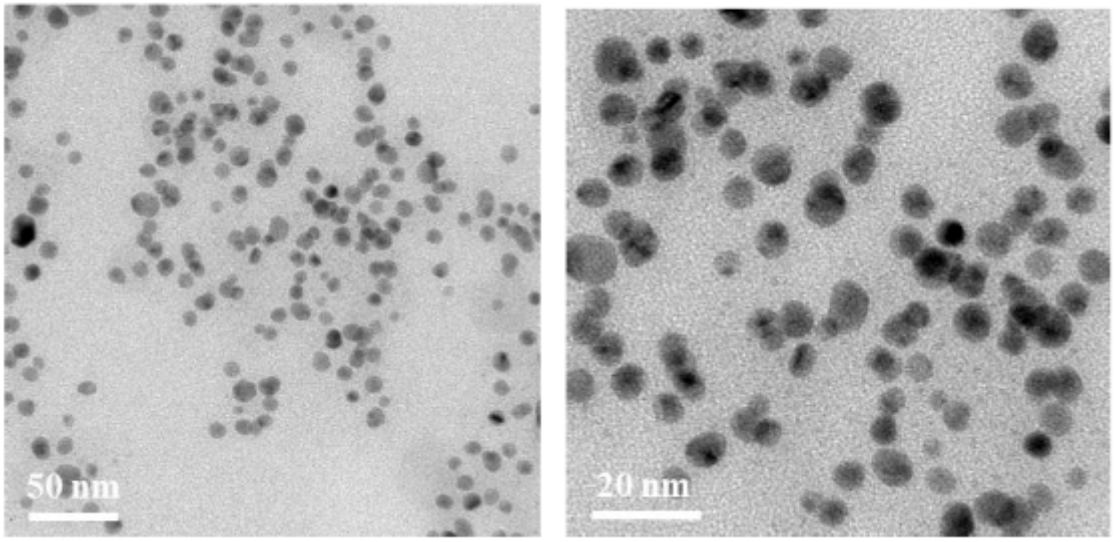

Figure 6. Representative transmission electron microscope (TEM) images of as-prepared AgNPs produced under an irradiation time of 9 h.

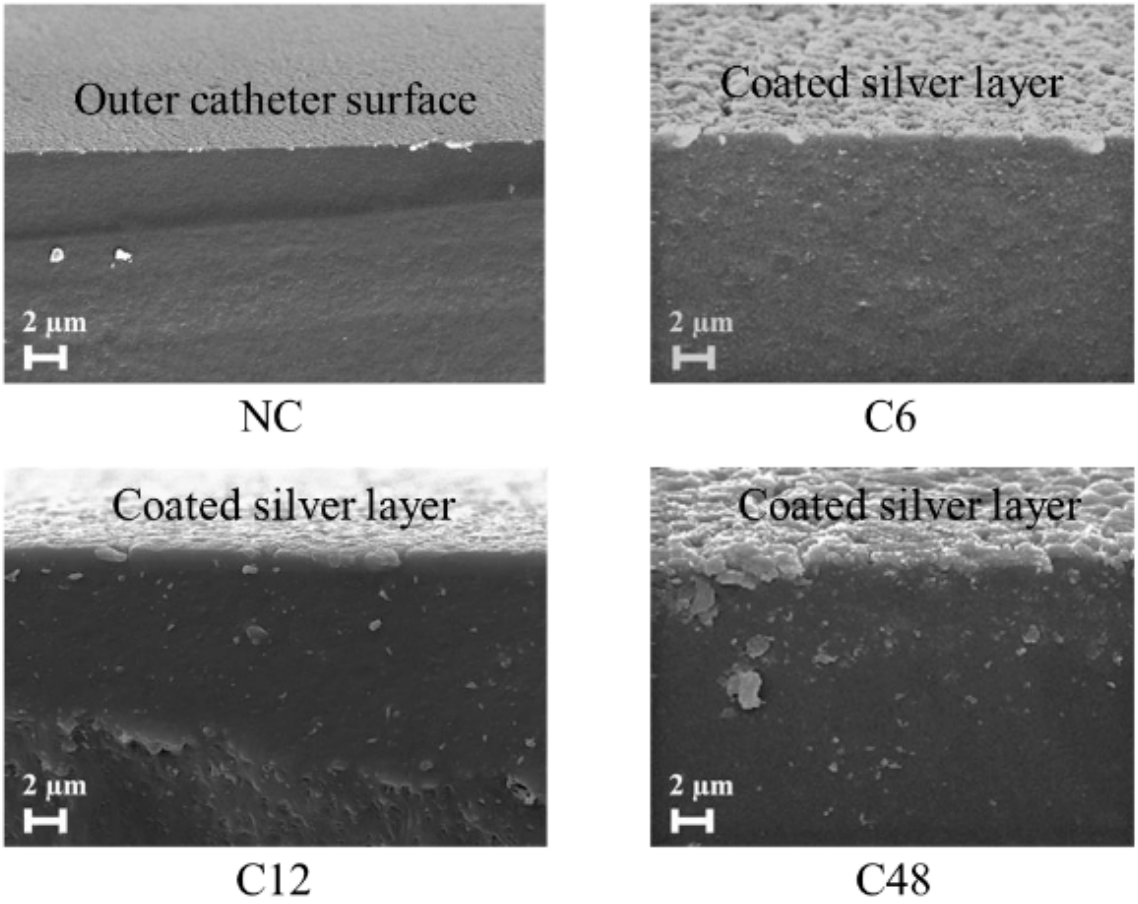

Figure 7. Cross-sectional field emission scanning electron microscope (FESEM) micrographs of NC, C6, C12, and C48.

Table 1. The summarized results providing the relationship between the silver content and *E. coli* mortality percentage.

Sample	Silver Content Coated on the Catheter Surfaces (mg/cm^2)	Mortality Rate (%)	Relative Mortality Rate (%/mg·cm^{-2})
C3	0.549	47	86
C12	0.637	82	129
C24	0.643	84	130
C48	0.712	91	128
CC	5.165	91	18

The antibacterial efficiency of 2 cm C48 was equivalent to the CC of the same length with a mortality rate of 91%, despite comprising a lower silver concentration. This behavior might occur from the excellent antibacterial properties of spherical AgNPs, which are smaller than 10 nm and show a high bacterial cytotoxicity due to their large surface area [36,37]. Whereas the relative mortality rate, from this point of view, showed insignificant differences in C12, C24, and C48 indicating a highly reproducible antibacterial catheter using the presented technique.

The possible cause underlying the lethal effect of AgNPs on *E. coli* cells was monitored using TEM analysis. Figure 9 shows the action of AgNPs on the cell membrane. We found that the cell membranes of native *E. coli* were smooth, while the membrane of cells treated with AgNPs coated on C48 were severely damaged, especially in the outer membrane, which resulted mainly from the direct AgNP-cell contact. At the contact site, the AgNPs interacted with lipids and lipopolysaccharide

molecules of the bacterial cell membrane, disrupting the bacterial membrane via membrane fluidization and altering the membrane permeability. Subsequently, the AgNPs were able to penetrate inside the bacteria after a few minutes in contact through the membrane pores, leading to interactions with biomolecules, such as proteins, lipids, and DNA. This interaction is followed by the denaturation of proteins causing uncontrolled transport through the plasma membrane, cell lysis, and eventually cell death [22,27,36,38–41].

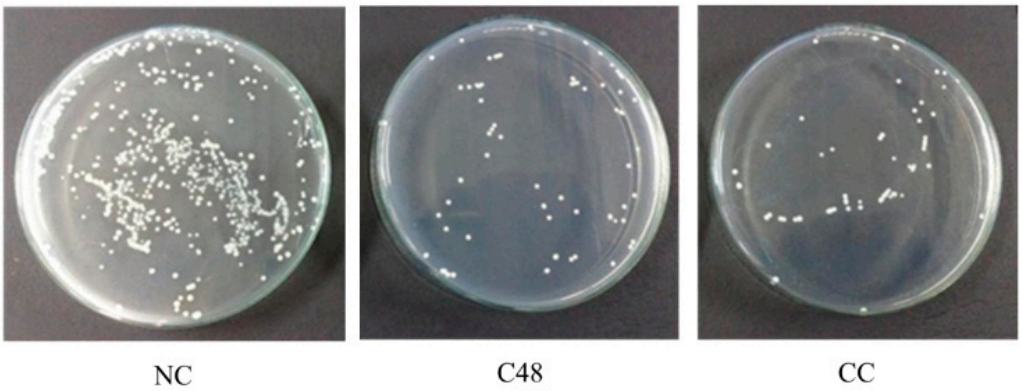

Figure 8. Plate-counting analysis of bactericidal activity of the urinary catheters before and after coating with AgNPs under the photo-irradiation time of 48 h and the purchased commercial antibacterial urinary catheters.

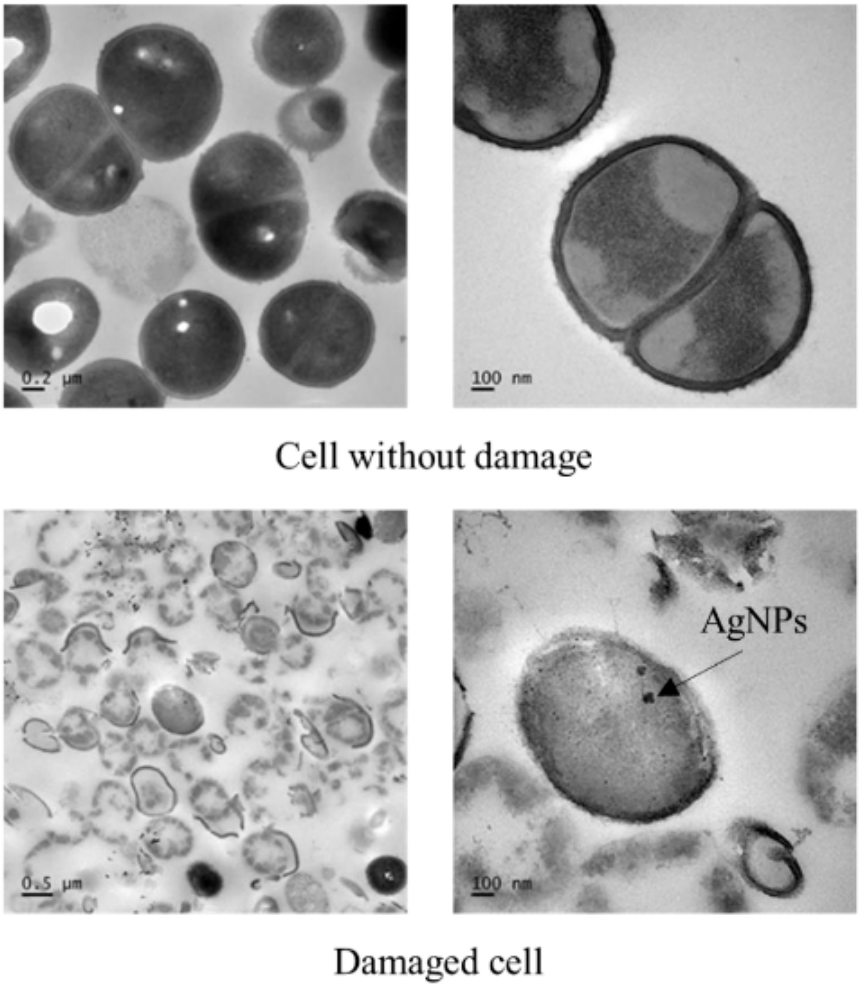

Figure 9. The effects of AgNPs on cell membranes of *E. coli* observed by TEM analysis.

3.3. In Vitro Study of Silver Released from Coated Catheter

As mentioned above, the bactericidal effect of AgNPs might be divided into two possibilities, one being the responsibility of silver ions released from AgNPs. To mimic real situations, the time-dependent release rate of silver ions from the AgNPs coated catheter into artificial urine (pH 7.4) was investigated using ICP-OES measurements. Based on the above results, the catheter coated AgNPs for 48 h in 2 cm long segments were chosen as samples in this section due to the high bactericidal activity (yield 91%), equivalent to the commercial antimicrobial catheter.

Figure 10 shows the in vitro silver release kinetic from the C48 catheter. We found that the cumulative amount of silver released in the artificial urine over 10 days was about 0.040 μg/mL, which was lower than the silver concentration considered for human tissue and organ toxicity [42]. From the results of the silver content coated on the catheters and silver release test, this, therefore, indicated that a major antibacterial effect of the AgNPs coated catheter developed herein was the direct adhesion interaction between AgNPs and the bacterial cell membranes according to the possible mechanistic details described in the previous section.

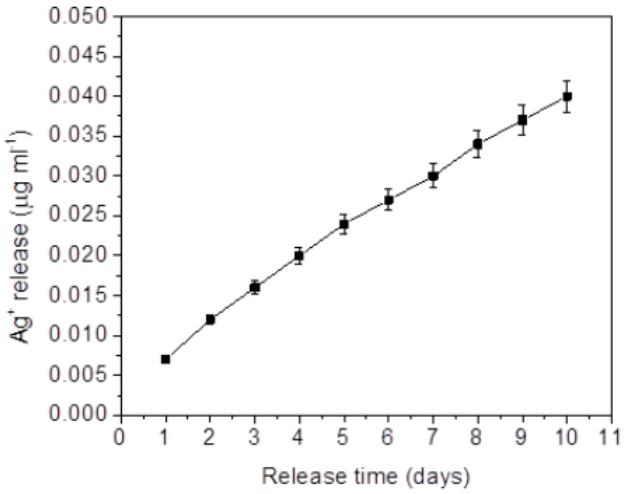

Figure 10. Time-dependent silver ion (Ag^+) release from the developed antibacterial urinary catheter prepared under the irradiation time of 48 h. Each data point represents the average cumulative daily content of silver released in μg/mL.

4. Conclusions

From the present investigation, the results clearly demonstrated that the antibacterial urinary catheter was successfully prepared using the novel in situ photo-assisted deposition method, which overcame the other complicated multi-step procedures. AgNPs of 9 nm diameter with strong antibacterial efficiency as bioactive coatings were prepared and simultaneously deposited on the catheter surfaces using durian rind waste as a natural precursor. This is an efficient alternative waste management strategy for the utilization of the abundant agro-industrial wastes to manufacture cost-effective antimicrobial medical devices to fight against uropathogens. The antibacterial activity against the drug-resistant pathogen, carbapenem-resistant uropathogenic *Enterobacteriaceae*, is being studied by our research group, and the results are expected to be presented in the near future.

Author Contributions: Conceptualization, F.C. and K.T.; methodology, K.T.; validation, F.C.; data curation, F.C.; writing—original draft preparation, K.T.; writing—review and editing, F.C.; supervision, P.L. and S.T. All authors have read and agreed to the published version of the manuscript.

Funding: This research was funded by Science Achievement Scholarship of Thailand.

Acknowledgments: The authors would like to thank National Nanotechnology Center, National Science and Technology Development Agency for providing the FESEM measurements.

Conflicts of Interest: The authors declare no conflict of interest.

References

1. Collins, A.S. Preventing Health Care-Associated Infections. In *Patient Safety and Quality: An Evidence-Based Handbook for Nurses*; Hughes, R.G., Ed.; Agency for Healthcare Research and Quality: Rockville, MD, USA, 2008; Volume 1, pp. 1–29.
2. Flores-Mireles, A.L.; Walker, J.N.; Caparon, M.; Hultgren, S.J. Urinary Tract Infections: Epidemiology, Mechanisms of Infection and Treatment Options. *Nat. Rev. Microbiol.* **2015**, *13*, 269–284. [CrossRef]
3. Anjum, S.; Singh, S.; Benedicte, L.; Roger, P.; Panigrahi, M.; Gupta, B. Biomodification Strategies for the Development of Antimicrobial Urinary Catheters: Overview and Advances. *Glob. Chall.* **2017**, *2*, 1700068. [CrossRef]
4. Yassin, M.A.; Elkhooly, T.A.; Elsherbiny, S.M.; Reicha, F.M.; Shokeir, A.A. Facile Coating of Urinary Catheter with Bio-Inspired Antibacterial Coating. *Heliyon* **2019**, *5*, e02986. [CrossRef]
5. Albu, S.; Voidazan, S.; Bilca, D.; Badiu, M.; Truţă, A.; Ciorea, M.; Ichim, A.; Luca, D.; Moldovan, G. Bacteriuria and Asymptomatic Infection in Chronic Patients with Indwelling Urinary Catheter. *Medicine (Baltimore)* **2018**, *97*, e11796. [CrossRef]
6. Mukhit Kazi, M.; Harshe, A.; Sale, H.; Mane, D.; Yande, M.; Chabukswar, S. Catheter Associated Urinary Tract Infections (CAUTI) and Antibiotic Sensitivity Pattern from Confirmed Cases of CAUTI in a Tertiary Care Hospital: A Prospective Study. *Clin. Microbiol.* **2015**, *4*, 1000193. [CrossRef]
7. Wang, L.; Zhang, S.; Keatch, R.; Corner, G.; Nabi, G.; Murdoch, S.; Davidson, F.; Zhao, Q. In-vitro Antibacterial and Anti-Encrustation Performance of Silver-Polytetrafluoroethylene Nanocomposite Coated Urinary Catheters. *J. Hosp. Infect.* **2019**, *103*, 55–63. [CrossRef] [PubMed]
8. Marklew, A. Urinary Catheter Care in the Intensive Care Unit. *Nurs. Crit. Care* **2004**, *9*, 21–27. [CrossRef]
9. Gould, C.V.; Umscheid, C.A.; Agarwal, R.K.; Kuntz, G.; Pegues, D.A. Guideline for Prevention of Catheter-Associated Urinary Tract Infections 2009. *Infect. Control Hosp. Epidemiol.* **2010**, *31*, 319–326. [CrossRef] [PubMed]
10. Warren, J.W. Catheter-Associated Urinary Tract Infections. *Int. J. Antimicrob. Agents* **2001**, *17*, 299–303. [CrossRef]
11. Fernandez, R.S.; Griffiths, R.D. Duration of Short-Term Indwelling Catheters: A Systematic Review of the Evidence. *J. Wound Ostomy Cont. Nurs.* **2006**, *33*, 145–153. [CrossRef]
12. Kumar, C.G.; Sujitha, P. Green Synthesis of Kocuran-Functionalized Silver Glyconanoparticles for Use as Antibiofilm Coatings on Silicone Urethral Catheters. *Nanotechnology* **2014**, *25*, 325101. [CrossRef] [PubMed]
13. Trautner, B.W.; Darouiche, R.O. Catheter-Associated Infections: Pathogenesis Affects Prevention. *Arch. Intern. Med.* **2004**, *164*, 842–850. [CrossRef]
14. Neoh, K.G.; Li, M.; Kang, E.-T.; Chiong, E.; Tambyah, P.A. Surface Modification Strategies for Combating Catheter-Related Complications: Recent Advances and Challenges. *J. Mater. Chem. B* **2017**, *5*, 2045–2067. [CrossRef] [PubMed]
15. Pollini, M.; Paladini, F.; Catalano, M.; Taurino, A.; Licciulli, A.; Maffezzoli, A.; Sannino, A. Antibacterial Coatings on Haemodialysis Catheters by Photochemical Deposition of Silver Nanoparticles. *J. Mater. Sci. Mater. Med.* **2011**, *22*, 2005–2012. [CrossRef]
16. Charnley, M.; Textor, M.; Acikgoz, C. Designed Polymer Structures with Antifouling-Antimicrobial Properties. *React. Funct. Polym.* **2011**, *71*, 329–334. [CrossRef]
17. Roe, D.; Karandikar, B.; Bonn-Savage, N.; Gibbins, B.; Roullet, J.-B. Antimicrobial Surface Functionalization of Plastic Catheters by Silver Nanoparticles. *J. Antimicrob. Chemother.* **2008**, *61*, 869–876. [CrossRef]
18. Al-Qahtani, M.; Safan, A.; Jassim, G.; Abadla, S. Efficacy of Anti-Microbial Catheters in Preventing Catheter Associated Urinary Tract Infections in Hospitalized Patients: A Review on Recent Updates. *J. Infect. Public Health* **2019**, *12*, 760–766. [CrossRef]
19. Martins, K.B.; Ferreira, A.M.; Pereira, V.C.; Pinheiro, L.; Oliveira, A.d.; Cunha, M.d.L.R.d.S.d. In vitro Effects of Antimicrobial Agents on Planktonic and Biofilm Forms of *Staphylococcus saprophyticus* Isolated from Patients with Urinary Tract Infections. *Front. Microbiol.* **2019**, *10*, 40. [CrossRef]
20. Singha, P.; Locklin, J.; Handa, H. A Review of the Recent Advances in Antimicrobial Coatings for Urinary Catheters. *Acta Biomater.* **2017**, *50*, 20–40. [CrossRef]
21. Rai, M.K.; Deshmukh, S.D.; Ingle, A.P.; Gade, A.K. Silver Nanoparticles: The Powerful Nanoweapon against Multidrug-Resistant Bacteria. *J. Appl. Microbiol.* **2012**, *112*, 841–852. [CrossRef]

22. Li, W.-R.; Xie, X.-B.; Shi, Q.-S.; Zeng, H.-Y.; OU-Yang, Y.-S.; Chen, Y.-B. Antibacterial Activity and Mechanism of Silver Nanoparticles on *Escherichia coli*. *Appl. Microbiol. Biotechnol.* **2009**, *85*, 1115–1122. [CrossRef] [PubMed]
23. Burdușel, A.-C.; Gherasim, O.; Grumezescu, A.M.; Mogoantă, L.; Ficai, A.; Andronescu, E. Biomedical Applications of Silver Nanoparticles: An Up-to-Date Overview. *Nanomaterials* **2018**, *8*, 681. [CrossRef] [PubMed]
24. Sim, W.; Barnard, R.; Blaskovich, M.A.T.; Ziora, Z. Antimicrobial Silver in Medicinal and Consumer Applications: A Patent Review of the Past Decade (2007–2017). *Antibiotics* **2018**, *7*, 93. [CrossRef] [PubMed]
25. Raza, M.; Kanwal, Z.; Rauf, A.; Sabri, A.; Riaz, S.; Naseem, S. Size- and Shape-Dependent Antibacterial Studies of Silver Nanoparticles Synthesized by Wet Chemical Routes. *Nanomaterials* **2016**, *6*, 74. [CrossRef]
26. Cheon, J.Y.; Kim, S.J.; Rhee, Y.H.; Kwon, O.H.; Park, W.H. Shape-Dependent Antimicrobial Activities of Silver Nanoparticles. *Int. J. Nanomed.* **2019**, *14*, 2773–2780. [CrossRef]
27. Morones, J.R.; Elechiguerra, J.L.; Camacho, A.; Holt, K.; Kouri, J.B.; Ramírez, J.T.; Yacaman, M.J. The Bactericidal Effect of Silver Nanoparticles. *Nanotechnology* **2005**, *16*, 2346–2353. [CrossRef]
28. Agnihotri, S.; Mukherji, S.; Mukherji, S. Size-Controlled Silver Nanoparticles Synthesized Over the Range 5–100 nm Using the Same Protocol and Their Antibacterial Efficacy. *RSC Adv.* **2014**, *4*, 3974–3983. [CrossRef]
29. Xu, L.; Wang, Y.-Y.; Huang, J.; Chen, C.-Y.; Wang, Z.-X.; Xie, H. Silver Nanoparticles: Synthesis, Medical Applications and Biosafety. *Theranostics* **2020**, *10*, 8996–9031. [CrossRef]
30. Majeed, S.; Joel, E.L.; Hasnain, M.S. Novel Green Approach for Synthesis of Metallic Nanoparticles and its Biomedical Application. *Recent Pat. Nanomed.* **2018**, *8*, 177–183. [CrossRef]
31. Chutrakulwong, F.; Thamaphat, K.; Limsuwan, P. Photo-Irradiation Induced Green Synthesis of Highly Stable Silver Nanoparticles Using Durian Rind Biomass: Effects of Light Intensity, Exposure Time and pH on Silver Nanoparticles Formation. *J. Phys. Commun.* **2020**, *4*, 095015. [CrossRef]
32. DIN EN 1616:1999. *Sterile Urethral Catheters for Single Use*; German Institute for Standardisation (Deutsches Institut für Normung): Berlin, Germany, 1999; pp. 1–16.
33. Chen, Y.; Ming, H. Review of Surface Plasmon Resonance and Localized Surface Plasmon Resonance Sensor. *Photonic Sens.* **2012**, *2*, 37–49. [CrossRef]
34. Rastogi, L.; Arunachalam, J. Sunlight Based Irradiation Strategy for Rapid Green Synthesis of Highly Stable Silver Nanoparticles Using Aqueous Garlic (*Allium sativum*) Extract and Their Antibacterial Potential. *Mater. Chem. Phys.* **2011**, *129*, 558–563. [CrossRef]
35. Maki, D.G.; Tambyah, P.A. Engineering out the Risk for Infection with Urinary Catheters. *Emerg. Infect. Dis.* **2001**, *7*, 342–347. [CrossRef] [PubMed]
36. Anees Ahmad, S.; Sachi Das, S.; Khatoon, A.; Tahir Ansari, M.; Afzal, M.; Saquib Hasnain, M.; Kumar Nayak, A. Bactericidal Activity of Silver Nanoparticles: A Mechanistic Review. *Mater. Sci. Energy Technol.* **2020**, *3*, 756–769.
37. Jeong, Y.; Lim, D.W.; Choi, J. Assessment of Size-Dependent Antimicrobial and Cytotoxic Properties of Silver Nanoparticles. *Adv. Mater. Sci. Eng.* **2014**, *2014*, 1–6. [CrossRef]
38. Joshi, A.S.; Singh, P.; Mijakovic, I. Interactions of Gold and Silver Nanoparticles with Bacterial Biofilms: Molecular Interactions behind Inhibition and Resistance. *Int. J. Mol. Sci.* **2020**, *21*, 7658. [CrossRef]
39. Dakal, T.C.; Kumar, A.; Majumdar, R.S.; Yadav, V. Mechanistic Basis of Anitimicrobial Actions of Silver Nanoparticles. *Front. Microbiol.* **2016**, *7*, 1831. [CrossRef]
40. Durán, N.; Marcato, P.D.; Conti, R.D.; Alves, O.L.; Costa, F.T.M.; Brocchi, M. Potential Use of Silver Nanoparticles on Pathogenic Bacteria, Their Toxicity and Possible Mechanisms of Action. *J. Braz. Chem. Soc.* **2010**, *21*, 949–959. [CrossRef]
41. Yin, I.X.; Zhang, J.; Zhao, I.S.; Mei, M.L.; Li, Q.; Chu, C.H. The Antibacterial Mechanism of Silver Nanoparticles and Its Application in Density. *Int. J. Nanomed.* **2020**, *15*, 2555–2562. [CrossRef]
42. Gopinath, P.; Gogoi, S.K.; Chattopadhyay, A.; Ghosh, S.S. Implications of Silver Nanoparticle Induced Cell Apoptosis for in vitro Gene Therapy. *Nanotechnology* **2008**, *19*, 075104. [CrossRef]

Publisher's Note: MDPI stays neutral with regard to jurisdictional claims in published maps and institutional affiliations.

© 2020 by the authors. Licensee MDPI, Basel, Switzerland. This article is an open access article distributed under the terms and conditions of the Creative Commons Attribution (CC BY) license (http://creativecommons.org/licenses/by/4.0/).